7. Probabilistic Stability Analysis (Reliability Analysis)

Key Concepts

Sliding stability analysis of concrete or embankment dams does not lend itself well to the event tree method in all cases, particularly under normal operating conditions. That is because stability, or lack thereof, results from an interaction between the applied loads, the pore pressures or uplift forces, and the shear strength. There is typically not a linear step-by-step progression for these factors, although changes in shear strength and/or drainage may occur with time. Therefore, it is helpful to obtain some analytical information about the probability of failure (or unsatisfactory performance). This information can be used to estimate a range in the probability of sliding for event tree nodes (see section on Event Trees) representing various loading conditions.

The traditional factor of safety approach provides some insight into failure probability; typically conservative input values (shear strength and water pressures) are used in the analyses, and if the resulting factor of safety satisfies established criteria, the likelihood of failure is low. How low is another question, and factor of safety by itself is not a good indication. This is seen in Figure 7-1, which shows the distributions of driving force and resisting force for two cases.

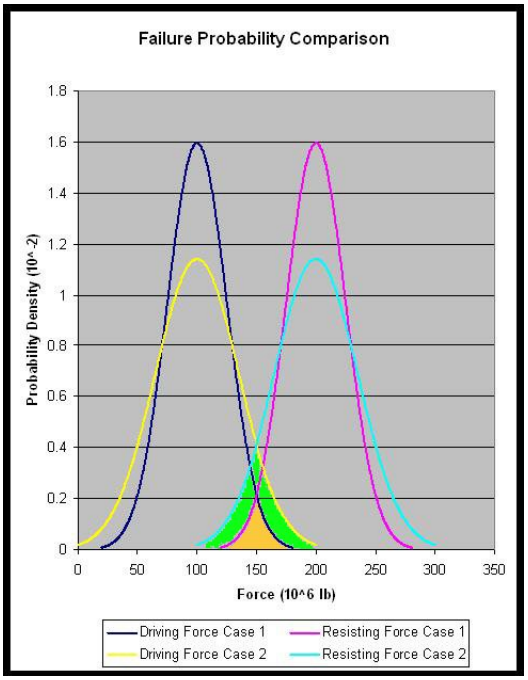

Figure 7-1. Factor of Safety and Failure Probability Comparison

The mean factor of safety (mean resisting force divided by mean driving force) is exactly the same for both cases. However, the probability of failure (area under

curves where the driving force is greater than the resisting force) is twice as high for the yellow and light blue curves (i.e. the orange area plus the green area) than it is for the dark blue and lavender curves (orange area).

With the development of new computer analysis tools; now, if you can program a deterministic analysis into a spreadsheet, you can use it to perform probabilistic analyses. This section describes the basic concepts of performing probabilistic analyses using a standard spreadsheet program (Microsoft ® Excel), and commercially available macro add-ins for probabilistic analysis (Palisade Corporation's @Risk). Other companies sell similar software (e.g. Lotus 1-2-3, and Crystal Ball by Decisioneering, Inc.). It should be noted that other analysis programs have the capability to perform reliability analysis (e.g. GRAVDAM for concrete gravity dams and SLOPE/W for embankment dams). However, these programs may not have the capability to display the sensitivity rank coefficients as described later, and hence some additional judgment may be needed when using these programs to perform sensitivity analyses. In addition, SLOPE/W will indicate a probability of failure equal to zero if none of the calculated factors of safety are less than 1.0. A reliability index is provided, but it is not clear what type of distribution is assumed in its calculation. GRAVDAM incorporates a cracked base analysis that must be used with caution (see also section on Concrete Gravity Dams)

The standard deterministic equations for calculating the factor of safety are programmed into a spreadsheet, but instead of defining the input parameters as single constant values, they are defined as distributions of values. Thus, instead of calculating a single value for the output factor of safety, a distribution of factor of safety is generated from numerous iterations using the so-called Monte-Carlo approach, whereby each of the input distributions are sampled in a manner consistent with their shape. This output distribution is used to determine the probability of safety factor less than that representing unsatisfactory performance.

For the purposes of this section of the manual, the probability of a factor of safety (FS) less than 1.0 is calculated. However, other values can be used (or the results tempered with judgment). For example, if the dam is particularly susceptible to deformation damage, a larger value of safety factor may appropriately define the state at which "unsatisfactory performance" occurs (El-Ramly et al, 2002), and the probability of being less than that value calculated.

Example Embankment Post-Liquefaction Stability

Consider the homogeneous embankment dam geometry shown in Figure 7-2. The dam is in a seismically active area. What appears to be a continuous clean sand layer, approximately four to six feet thick, was encountered in three borings, approximately eight feet below the dam-foundation contact. The minimum corrected $(N_1)_{60}$ blow count values encountered in this layer varied from 13 to 15 depending on the boring. The toe of the dike is wet, indicating a high phreatic surface and saturated foundation materials in that area. Piezometers installed in the embankment indicate differences in the phreatic surface of about nine feet

from one hole to another at the same distance downstream of the centerline. Given the sand layer liquefies, what is the probability of post-liquefaction instability?

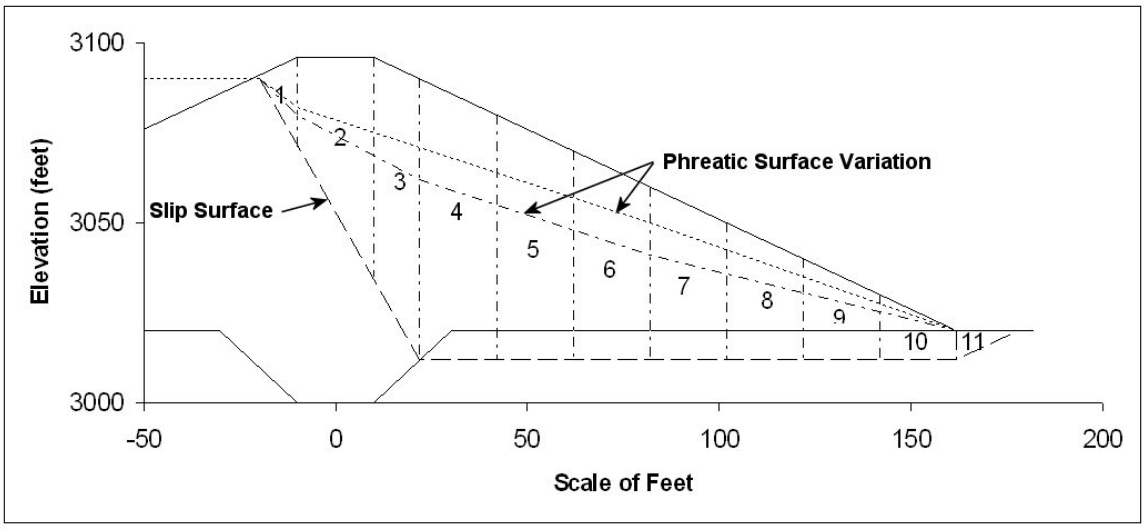

Figure 7-2. Example Embankment Dam Geometry

The sliding surface was assumed to follow the liquefied sand layer and intersect the upstream face below the reservoir surface at normal full pool, such that no embankment remnant would be left to retain the reservoir. Although there may be slip surfaces with a lower factor of safety, judgment is needed to select a surface that will not result in a crest remnant capable of retaining the reservoir. It may be appropriate to examine other slip surfaces, or use a factor of safety greater than 1.0 to represent unsatisfactory performance to cover the possibility of a more critical slip surface. The simplified Bishop method of analysis (Scott, 1974) was programmed into a spreadsheet, as shown in Figure 7-3. The "allow circular reference" feature in Excel is used to iterate to the solution. Eleven slices were used to define the potential sliding mass.

	A	B	C	D	E	F	G	H	I	J	K	L
1	Bishop's Slope Stability Analysis											
2												
3	Drained Strengths			Undrained Strengths			Density					
4	c' =	696	psf	c =	637	psf	γ =	114	pcf			
5	tan Φ' =	0.672		tan Φ =	0							
6	Φ' =	33.9	degrees	Φ =	0							
7												
8												
9	Slice	Δxi	c*Δxi	ui	ui*Δxi	Wi	θi	(Wi-ui*Δxi)*tanΦ	C + H	cos(θi)*[1+(tanθi*tanΦ/FS)]	I / J	Wi*sinθi
10		(ft)	(kips)	(ksf)	(kips)	(kips)	(deg)	(kips)				(kips)
11												
12	1	12	8.35	0.28	3.37	17.72	60.6	9.64	18.00	0.92	19.63	15.44
13	2	20	13.92	1.45	29.02	99.97	60.6	47.68	61.60	0.92	67.21	87.10
14	3	12	8.35	2.90	34.82	94.06	60.6	39.81	48.16	0.92	52.55	81.95
15	4	20	12.73	0	0.00	165.86	0.0	0.00	12.73	1.00	12.73	0.00
16	5	20	12.73	0	0.00	143.14	0.0	0.00	12.73	1.00	12.73	0.00
17	6	20	12.73	0	0.00	120.42	0.0	0.00	12.73	1.00	12.73	0.00
18	7	20	12.73	0	0.00	97.70	0.0	0.00	12.73	1.00	12.73	0.00
19	8	20	12.73	0	0.00	74.98	0.0	0.00	12.73	1.00	12.73	0.00
20	9	20	12.73	0	0.00	52.26	0.0	0.00	12.73	1.00	12.73	0.00
21	10	20	12.73	0	0.00	29.54	0.0	0.00	12.73	1.00	12.73	0.00
22	11	16	11.13	0.19	3.00	7.27	-26.6	2.87	14.01	0.68	20.74	-3.26
23										Sum ->	249.26	181.23
24	FS = ΣK/ΣL =	1.38										

Figure 7-3. Bishops Method of Slope Stability Analysis

Input variables defined as distributions include: (1) embankment soil unit weight (γ), (2) effective stress cohesion of the embankment material (c'), (3) effective stress friction angle of the embankment material (φ'), (4) undrained residual shear strength of the liquefied sand layer (S_u), and (5) water forces at the base of each embankment slice for which effective stress parameters were defined. No test results were available for the embankment materials. Therefore, the mean, standard deviation, maximum, and minimum values listed in *Design of Small Dams* (BOR, 1987) for SC material (see Table 7-1) were used to define truncated normal distributions. The @Risk function for the effective stress cohesion as an example, is RiskNormal(720,360,RiskTruncate(101,1224)). The friction angles were converted to tan φ' for the spreadsheet calculations. It should be noted that in many cases these types of embankment materials are treated as undrained, or "friction only" strengths are used based on the shear strength curves. However, both c' and φ' are used in this example for illustration purposes.

Table 7-1. Summary of embankment input properties

Property	Minimum	Maximum	Mean	Standard Deviation
Moist Unit Weight (lb/ft^3)	91.1	131.8	115.6	14.1
c' (lb/ft^2)	101	1224	720	360
φ' (degrees)	28.4	38.3	33.9	2.9

For simplicity, moist soil unit weight was used for the entire soil mass, including the foundation alluvium. It is recognized that the saturated embankment unit weight (below the phreatic surface) will actually be slightly higher, and the alluvial materials could also be somewhat different. It is also assumed that the effective stress parameters listed in Table 7-1 are equally applicable above and below the phreatic surface.

A variation in phreatic surface of up to nine feet under the downstream face was used to estimate water pressures and forces at the base of each slice where the sliding surface passes through the embankment, as shown in Figure 7-2. A uniform distribution between the upper and lower values was assigned, for example RiskUniform(1.22,1.68) in $kips/ft^2$, indicating any value between the upper and lower value is equally likely.

Finally, undrained residual shear strength of the liquefied foundation sand was estimated using the curves developed by Seed and Harder (Seed et al, 2003). Upper and lower bound curves are provided as a function of corrected blow count. It was assumed that midway between the curves represented the best estimate value. A triangular distribution between the upper and lower bound values, with a peak at the best estimate was used to define this input parameter, RiskTriang(360,630,920) in lb/ft^2. It is recognized that more recent guidance suggests a relationship proposed by Olson and Stark (2002) should carry a small weight in combination with the Seed and Harder relationship (Seed et al, 2003).

However, it is expected the Seed and Harder relationship would be slightly more conservative, and for simplicity it was used alone.

After entering the input distributions in the spreadsheet cells, the factor of safety cell is selected as the output and the simulation settings are adjusted. In this case, 10,000 iterations were specified using the Latin Hypercube sampling method. Using the Latin Hypercube method just means that the same combination of values is not selected more than once, and the results should converge to a smooth distribution more quickly. Then the simulation is run with the click of a button. For each iteration, the input distributions are sampled in a manner consistent with their shape or probability density function, and a factor of safety is calculated. This results in a listing of the calculated factors of safety for the simulation. It is a simple matter to sort the listing of output factors of safety in ascending or descending order using the sort command of the spreadsheet program. The probability of FS<1.0 is the number of iterations whose calculated factor of safety is less than 1.0, divided by the total number of iterations. In this case 228 iterations produced a factor of safety less than 1.0. Therefore, the probability of FS<1.0 is 228/10,000 or 0.0228.

To help understand which input distributions have the greatest effect on the results, the @Risk program prints out a list of ranking coefficients. Those input distributions with the highest positive or negative ranking coefficients affect the results most. For the example just described, the coefficients are shown in Table 7-2. It can be seen that the drained cohesion of the embankment, c', and the undrained residual shear strength of the sand layer, S_u, affect the results the most. A negative ranking coefficient just means that the variable is negatively correlated with the result. For example, an increase in water force results in a decrease in factor of safety, as expected.

Table 7-2. Embankment dam sensitivity rank coefficients

Rank	Name	Cell	Regression	Correlation
1	c'	B4	0.726344	0.732725132
2	S_u	E4	0.590719261	0.575407848
3	γ	H4	-0.292465055	-0.272376816
4	φ'	B5	0.137192535	0.130003719
5	u slice 2	D13	-0.072522808	-0.070526537
6	u slice 3	D14	-0.052556307	-0.051631753
7	u slice 11	D22	-0.020666858	-0.020920598
8	u slice 1	D12	-0.018467738	-0.004675745

Although probabilistic analyses attempt to account for uncertainty, when dealing with dam safety engineering it is unlikely there will be sufficient data to define the input distributions with extreme confidence. Therefore, it may be appropriate to perform sensitivity studies using variations to the input distributions. For the case of the slope described above, two additional simulations were run with the following variations:

- Examination of test values for SM soils from *Design of Small Dams* (BOR, 1987) indicates a higher mean and more variation in c' than for SC material. Since some siltier zones were observed in the embankment during sampling, more variation in this property may be warranted. However, the mean value used appears to be appropriate. The standard deviation of the drained embankment cohesion, c', was increased by 50 percent to 540 lb/ft^2. In addition, rather than truncating the maximum and minimum values for c' at the soil test values shown in Table 1, these values were allowed to vary between 20 and 2000 lb/ft^2 to account for the fact that the full range of possible values may not have been captured by the limited testing.
- In lieu of No. 1 above, the undrained residual strength of the sand layer was taken as RiskTriang(310,560,790) based on an $(N_1)_{60}$ value of 13 (lower value from the exploration) rather than 14 (mid-range value).

The results of all three simulations are summarized in Table 7-3. Increasing the standard deviation and upper limit for c' also increased the location of the distribution centroid, resulting in a higher mean factor of safety. However, it can be seen that, although the mean factor of safety increased when more variation was allowed, the probability of FS<1.0 also increased. Decreasing the residual undrained shear strength of the sand layer decreased the mean factor of safety and increased the probability of FS<1.0 as expected. These analyses provide a quantitative indication of what this actually means in terms of failure likelihood for the embankment studied. They also provide an indication of the likely range in failure probability, given uncertainty in the input distributions. It should be noted that even if the embankment remains stable, deformations could result in transverse cracking through which seepage erosion could take place. This must also be considered in evaluating the overall risks posed by the dam and reservoir.

Table 7-3. Results of embankment post-liquefaction simulations

Case	Mean F.S.	Probability F.S.<1.0
Original Input Distributions	1.38	0.0228
Increase Std Dev and Limits	1.44	0.0345
Lower Undrained Residual Strength	1.32	0.0605

Example RCC Dam Stability

The method is equally applicable for sliding of concrete structures. For example, construction of a 160-foot-high roller-compacted concrete (RCC) dam in a wide canyon was suspended for winter shut down after the RCC reached a height of 20 feet. The following construction season, the cold joint surface of the previous year was thoroughly cleaned and coated with mortar, and the remainder of the dam was placed. A gallery was constructed such that the gallery floor would be about 5 feet above tailwater during PMF conditions. A line of three-inch-diameter drains, spaced at 10 feet, was angled downstream from the gallery, intersecting the cold joint about 28 feet downstream of the axis. Although a 3.5-

foot-high parapet wall was constructed on the upstream side of the dam crest, the spillway was sized to pass the probable maximum flood (PMF) without encroaching on the wall. Due to concerns about the strength of the cold joint, five six-inch diameter cores were taken one year later. Two of the five cores were not bonded at the lift joint. The remaining three were tested in direct shear at varying normal stresses. Although only three data points were generated, the results were well behaved as shown in Figure 7-4. Accounting for about 40 percent de-bonded area of the joint, it was determined that the design intent was still met. Several years later, the PMF was revised and a flood-frequency analysis was performed. Although the new PMF did not overtop the dam, it encroached about 2.3 feet onto the parapet wall. Maximum tailwater did not change significantly. Additional stability analyses were undertaken to evaluate the likelihood of failure under the new loading condition.

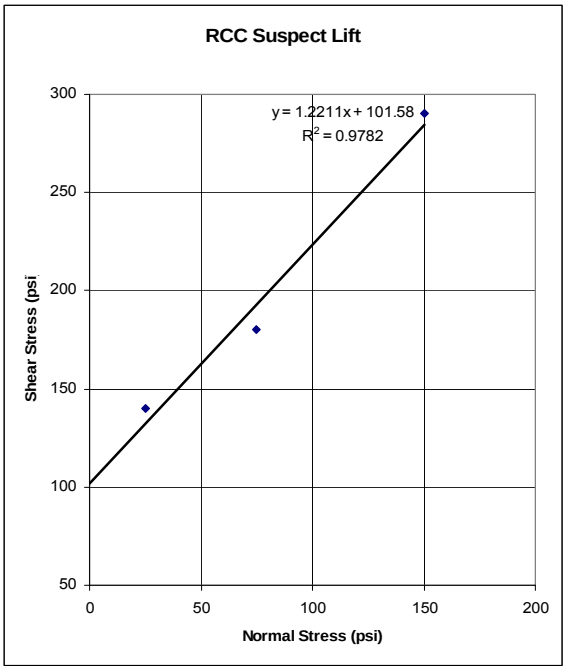

Figure 7-4. Direct shear test results for suspect RCC lift joint

The section shown in Figure 7-5 was used in the analysis. The vertical stress at the upstream face is calculated considering the familiar standard equation from mechanics of materials: P/A +/- Mc/I to account for the vertical load (P) and the moment (M) induced by the reservoir for the total stress condition, as indicated by Watermeyer (2006). Initially, uplift is approximated by a bi-linear distribution, varying from full reservoir pressure at the upstream face, to a reduced pressure at the line of drains, to tailwater at the downstream face. The total head at the line of drains is defined as F_d * (Reservoir El. – Tailwater El.) + Tailwater El., where F_d is the drain factor (1-efficiency). The pressure head is determined by subtracting the elevation of the potential sliding surface from the total head. The effective stress is calculated along the potential sliding plane by subtracting the uplift pressure from the total stress, and where the effective stress is calculated to

be tensile, no resistance is included for that portion of the plane. Since the locations of potential joint de-bonding are unknown, the cold joint was also assumed to be cracked to the point of zero effective stress in this case. Full uplift was assumed in the crack until it extended past the drains. Then, approximate equations were used to adjust the drain factor to account for the crack length, based on research performed at the University of Colorado (Amadei et al, 1991). This required the "allow circular reference" feature of Excel to iterate on a crack length. The factor of safety was then ultimately calculated from the familiar equation FS = [c'A + (W-U)tanφ']/D, where W is the vertical load, A is the bonded area, U is the uplift force, and D is the driving force taking into account both the downstream-directed reservoir load and the upstream-directed tailwater load.

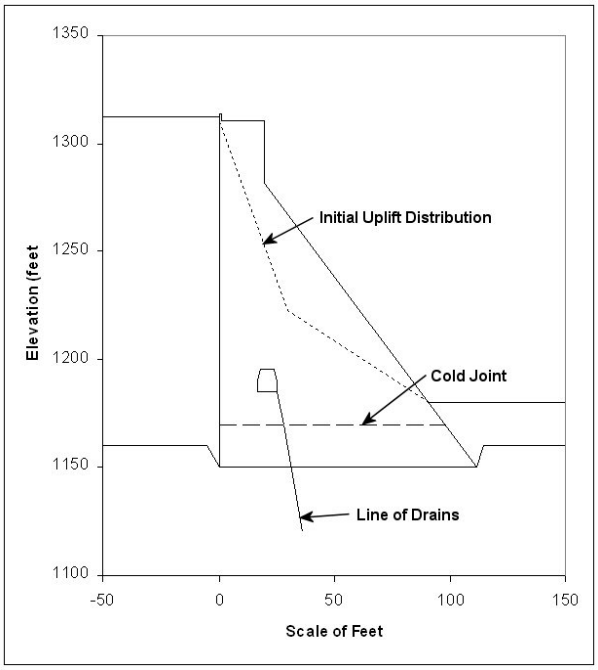

Figure 7-5. Geometry of RCC gravity dam

The equations for limit equilibrium analysis were programmed into a spreadsheet. Input variables that were defined as distributions included the following: (1) drain factor F_d, (2) tangent of the intact friction angle on the potentially weak lift joint φ', (3) intact cohesion on the potentially weak lift joint c', (4) percent of the joint that is intact, and (4) the RCC density. Table 7-4 defines the distributions that were used.

The RCC density, based on measurements from the core, was relatively constant, and a uniform distribution between the minimum and maximum values was used.

- The initial drain factor was taken to be a uniform distribution based on piezometer measurements and experience with other concrete dams of similar geometry.
- The coring would suggest that about 60 percent of the lift surface was bonded, assuming the cores were not mechanically broken during drilling.

To estimate a likely range, the percentage was adjusted assuming the drilling of two more holes yielded bonded lifts on the high side, or yielded unbonded lifts on the low side.

- Both the cohesion and tangent friction angle were defined as triangular distributions, with the peak of the distribution corresponding to the straight line fit shown in Figure 3. High and low values were estimated based on experience with other direct shear tests on concrete joints, and passing reasonable lines through the data points.

Table 7-4. Summary of concrete input properties

Property	Distribution	Minimum	Peak	Maximum
Initial Drain Factor, F_d	Uniform	0.33	n/a	0.75
φ' (degrees)	Triangular	43	50	57
Intact c' (lb/in^2)	Triangular	50	100	150
Percent Intact	Triangular	43	60	71
Density (lb/ft^3)	Uniform	146	n/a	152

The minimum safety factor calculated from 10,000 iterations was 1.43, with a mean value of 2.42. The sensitivity analysis indicated the cohesion had the largest effect on the results as shown in Table 7-5.

Table 7-5. RCC dam sensitivity rankings

Rank	Name	Cell	Regression	Correlation
1	Intact Cohesion (psi) =	B17	0.759017659	0.759702063
2	TAN Friction Angle =	B16	0.411501707	0.395787559
3	Percent Intact =	B18	0.368619688	0.349212338
4	Drain Factor =	B15	-0.311968848	-0.314501945
5	Concrete Density (pcf) =	B19	0.09730957	0.085434774

Figure 7-4 suggests that the cohesion and friction angle are negatively correlated. That is, as the friction angle becomes greater, a line that passes through the data would intercept the vertical axis at a lower cohesion value, and vice versa. @Risk allows the user to correlate input variables, such that in this case, a high value of cohesion will only be sampled with a low value of friction angle, and vice versa. Since there were limited data points upon which to base a correlation, a negative correlation coefficient of 0.8 was selected, meaning that the highest cohesion value doesn't have to be associated with the absolute lowest friction angle, but the general trend of the correlation is maintained. The minimum factor of safety calculated with this correlation is 1.79, higher than if the correlation is not maintained, indicating that ignoring the correlation would be conservative.

Since the factor of safety never drops below 1.0, it is not possible to determine the probability of FS<1.0 in the same manner as for the embankment dam example. Since none of the 10,000 iterations produced a FS<1.0, it can be said that the probability of FS<1.0 is less than 1 in 10,000. However, it is possible to estimate

a probability of FS<1.0 by fitting a distribution to the results without needing to run millions of iterations.

For this, the parameter "reliability index" or β must be introduced. The reliability index is simply the "number of standard deviation units" between the mean value and value representing failure. Figure 7-6 shows the output factor of safety distribution for the first case discussed for the RCC gravity dam; with cohesion and friction angle treated as independent variables. Goodness of fit tests indicate the distribution follows a normal (bell-shaped) distribution quite well. The reliability index in this case, relative to a safety factor of 1.0, is $(FS_{AVG} - 1.0)/\sigma_F$, where FS_{AVG} is the mean safety factor and σ_F is the standard deviation of the safety factor distribution, or $\beta = (2.425\text{-}1.0)/0.3126 = 4.56$. There is a standard function in Microsoft Excel that allows one to estimate the probability of FS<1.0 directly from the reliability index, which is 1-NORMSDIST(β). In this case, using this function produces a probability of FS<1.0 of 2.61×10^{-6}. This is a very low number, which seems reasonable given the high mean factor of safety and the fact that the minimum value calculated in 10,000 iterations never dropped below 1.4. In many cases, the output factor of safeties may not follow a normal distribution, but rather a lognormal distribution. This same method can be used to estimate the probability of FS<1.0. The only difference is that the reliability index is calculated with a different formula (Scott et al, 2001), as follows:

$$\beta_{\log normal} = \frac{\ln\left(\frac{FS_{mean}}{\sqrt{1+V_{FS}^2}}\right)}{\sqrt{\ln\left(1+V_{FS}^2\right)}}$$

Where FS_{mean} is the average factor of safety and V_{FS} is the coefficient of variation for the factor of safety, equal to the standard deviation divided by the mean. In some cases, BestFit (another computer program by Palisade Corporation) can be used to estimate the area under the tails of the distribution (at values less than 1.0) directly from the distribution by moving the cursor to 1.0 and reading the percentage of the distribution under the area to the left of that point.

Note: for very long potential failure surfaces through a given material, the strength parameters may not be consistent all along the surface. The "spatial variability" can be accounted for by dividing the surface into representative segments (perhaps based on spacing of test information) and separate input distributions defined for each segment.

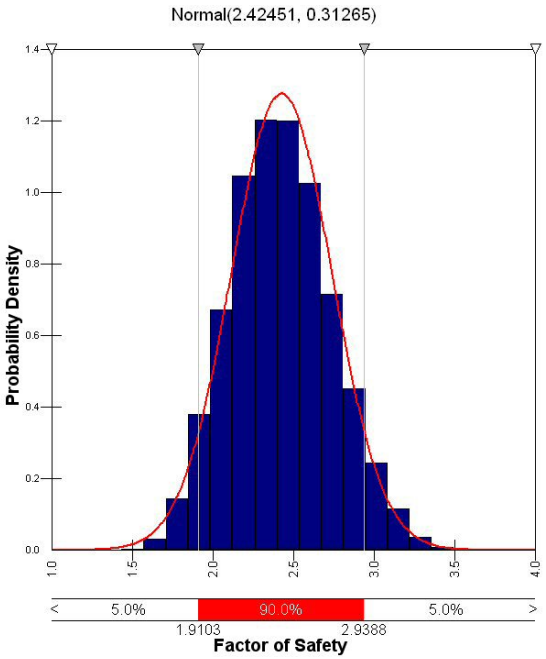

Figure 7-6. Output factor of safety distribution for RCC dam

Using Reliability Analysis within a Risk Analysis

The type of probabilistic stability analysis described in the preceding paragraphs is sometimes referred to as "reliability analysis". It is important to note that Reclamation does not typically use reliability analysis as the sole method for estimating failure probability. However, when appropriate models are available, they can be a useful tool in estimating response components or "conditional" probabilities (probabilities that are conditional upon given loadings or states). That is, given the loading condition (e.g. reservoir level or earthquake) and state (e.g. liquefied foundation) they help define the failure probability. This may occur for one or more branches of a fairly complex event tree. The annual probability of failure is the probability of the loading multiplied by the probability of failure given the loading. Reliability analysis has been used as a component in the risk analyses for a variety of structures, including Folsom (concrete gravity) Dam, Upper Stillwater (RCC gravity dam), Pueblo (concrete buttress dam) and for estimating construction risks with an excavation at the toe of Mormon Island Auxiliary (embankment) Dam.

Model Uncertainty

The preceding discussion provides a method for calculating probabilities considering uncertainties in the input parameters. This type of uncertainty is sometimes referred to as parameter uncertainty. However, significant uncertainty also exists as to how well the models used in the calculations actually reflect the real situation. This is sometimes referred to as model uncertainty. Models are just that, limited approximations. Vick (2002) provides additional discussion concerning limitations of models. The models used in the spreadsheet

calculations previously described are two-dimensional simplifications of complex three-dimensional problems. It may be appropriate to modify the results of the numerical reliability analyses based on subjective degree of belief (see Section on Subjective Probability and Expert Elicitation). For example, if there are significant three-dimensional effects that tend to help with stability, but a complex three-dimensional analysis is not available, the failure probability can be reduced based on the expectations related to 3-D improvements to stability. Similarly, if there are uncertainties in the model that are unconservative or questionable, such as whether shear strengths will be mobilized at the same shear strains for different materials along the sliding plane, the failure probability can be increased.

Considerations for Comprehensive Facility Review

Since this type of analysis typically takes a bit of time to perform, it is seldom used at the Comprehensive Facility Review (CFR) level. CFR's rely more heavily on subjective probabilities (see Section on Subjective Probability and Expert Elicitation).

Exercise

Consider a rock block resting on a joint plane. Statistical evaluation of the joint data indicates a mean dip of 27 degrees with a standard deviation of 6 degrees. Direct shear tests suggest a mean friction angle of 34 degrees with a standard deviation of 8 degrees. Calculate the probability of block sliding (factor of safety less than 1.0) assuming the slope is dry.

References

Amadei, B., T. Illangasekare, C. Chinnaswamy, D.I. Morris, "Estimating Uplift in Cracks in Concrete Dams," Proceedings, International Conference on Hydropower, Denver, Colrado, July 24-26, 1991.

Bureau of Reclamation, *Design of Small Dams*, Third Edition, Denver, CO, 1987.

El-Ramly, H., N.R. Morgenstern, and D.M. Cruden, "Probabilistic Slope Stability Analysis for Practice," *Canadian Geotechnical Journal*, NRC Canada, Volume 39, pp. 665-683, 2002.

Olson, S. M. & Stark, T. D, "Liquefied strength ratio from liquefaction case histories," Canadian Geotechnical Journal, Volume 39, No. 3, pp 629–647, March, 2002.

Seed, R.B., K.O. Cetin, R.E.S. Moss, A.M. Kammerer, J. Wu, J.M. Pestana, M.F. Riemer, R.B. Sancio, J.D. Bray, R.E. Kayen, and A. Faris, "Recent Advances in Soil Liquefaction Engineering: A Unified and Consistent Framework," 26th Annual ASCE Los Angeles Geotechnical Spring Seminar, Long Beach, CA, April 30, 2003.

Scott, C.R., *Soil Mechanics and Foundations*, Applied Science Publishers, Ltd., London, Second Edition, 1974.

Scott, G.A., J.T. Kottenstette, and J.F. Steighner, "Design and Analysis of Foundation Modifications for a Buttress Dam," *Proceedings, 38th U.S. Symposium on Rock Mechanics*, Washington, DC, A.A. Balkema, pp. 951-957, 2001.

Scott, G.A. "Probabilistic Stability Analysis – You Can Do It," Proceedings, Association of State Dam Safety Officials Conference, Austin, Texas, 2007.

Vick, S.G., *Degrees of Belief, Subjective Probability and Engineering Judgment*, ASCE Press, Reston, VA, 2002.

Watermeyer, C.F., "A Review of the Classical Method of Design of Medium Height Gravity Dams and Aspects of Base Shortening with Uplift," *Journal of the South African Institution of Civil Engineering*, Vol 48 No 3, pp. 2-11, 2006.

This Page Left Blank Intentionally